A Consensus-Based Cooperative Control of PEV Battery and PV Active Power Curtailment for Voltage Regulation in Distribution Networks

Mehdi Zeraati, *Student Member, IEEE*, Mohamad Esmail Hamedani Golshan, and Josep M. Guerrero, *Fellow, IEEE*

***Abstract*—The rapid growth of rooftop photovoltaic (PV) arrays installed in residential houses leads to serious voltage quality problems in low voltage distribution networks (LVDNs). In this paper, a combined method using the battery energy management of plug-in electric vehicles (PEVs) and the active power curtailment of PV arrays is proposed to regulate voltage in LVDNs with high penetration level of PV resources. A distributed control strategy composed of two consensus algorithms is used to reach an effective utilization of limited storage capacity of PEV battery considering its power/capacity and state of charge. A consensus control algorithm is also developed to fairly share the required power curtailment among PVs during overvoltage periods. The main objective is to mitigate the voltage rise due to the reverse power flow and to compensate the voltage drop resulting from the peak load. Overall, the proposed algorithm contributes to a coordinated charging/discharging control of PEVs battery which provides a maximum utilization of available storage capacity throughout the network. In addition, the coordinated operation minimizes the required active power which is going to be curtailed from PV arrays. The effectiveness of the proposed control scheme is investigated on a typical three-phase four-wire LVDN in presence of PV resources and PEVs.**

***Index Terms*—Active power curtailment, consensus algorithm, LV distribution network, PEV, PV.**

I. Introduction

THE DEVELOPMENT of renewable energy resources and promotion of transportation electrification are two effective strategies to encounter global concerns about climate change which is caused by greenhouse gas emission. Therefore, the total installed capacity of photovoltaic (PV) and the number of plug-in electric vehicles (PEVs) increase dramatically in low voltage distribution networks (LVDNs) [1] and thus distribution network operators (DNOs) face new operational challenges [2].

Manuscript received February 14, 2017; revised June 7, 2017 and July 28, 2017; accepted September 1, 2017. Date of publication September 7, 2017; date of current version December 19, 2018. Paper no. TSG-00218-2017. *(Corresponding author: Mohamad Esmail Hamedani Golshan.)*

M. Zeraati and M. E. Hamedani Golshan are with the Department of Electrical and Computer Engineering, Isfahan University of Technology, Isfahan 84156-83111, Iran (e-mail: m.zeraati@ec.iut.ac.ir; hgolshan@cc.iut.ac.ir).

J. M. Guerrero is with the Department of Energy Technology, Aalborg University, 9220 Aalborg, Denmark (e-mail: joz@et.aau.dk).

Color versions of one or more of the figures in this paper are available online at http://ieeexplore.ieee.org.

Digital Object Identifier 10.1109/TSG.2017.2749623

A large amount of connected PV resources may cause reverse power flow in light load conditions which brings about undesirable effects on operation and voltage regulation of distribution networks [3]. This problem should be solved immediately in order to achieve high penetration levels in the next years. On the other hand, the number of PEVs connected to LVDNs is expected to increase rapidly in the near future. Therefore, different PEV charging/discharging strategies have been used for supporting the networks [4].

In addition, LVDNs are mostly of three-phase four-wire type in which PV resources and PEVs are not equally distributed between three phases of the distribution network. This will increase the load unbalance which results in serious problems including a rise in energy losses, and voltage unbalance while reducing PV hosting capacity of the network [5].

Different methods have been proposed in the literature to deal with the voltage rise problem resulting from reverse power flow in LVDNs with high PV penetration. The main strategies are on-load tap changing (OLTC) transformer [6], active power curtailment (APC) of PV systems [7], reactive power management [8], and energy storage systems [9]. Another solution for this problem can be attained through coordinated control of PV and PEV systems. By adding more flexibility to modern distribution network, the energy storage capability of PEV battery can be used to improve the feeder operation [10]–[12].

A. Motivation

According to recent statistical studies [13], the PEVs are used by the owners for a short period of time per day and mostly they are parked. In [14], it has been estimated about 90% and 50% the probabilities that a PEV is parked somewhere or in a house at midday, when the PV generations are at the maximum level, respectively. As a result, a practical and realistic solution may be to utilize the energy storage capability of PEV battery with the aim of storing the extra energy during peak periods of PV generation. On the other hand, vehicle to grid (V2G) technology allows consuming the energy stored in PEV battery to compensate the voltage drop during peak load periods. However, PEVs charging is required to be postponed until the late at night or the early morning when the network loads are low. This strategy not only prevents extreme stress on the network due to the simultaneous charging of PEVs,

but also provides an effective tool for voltage regulation in the LVDN.

B. Literature Review

Voltage regulation strategies in distribution networks using PV or PEV systems are generally classified into centralized [15], [16], local [17], [18], and distributed [19]–[21] control methods. The centralized methods require expensive high-bandwidth communication infrastructures that their reliability and security are vulnerable to a single point of failure. The local control strategies only depend on local measurements. Not needing a communication infrastructure is one of the main advantages of local methods. However, due to a lack of information about the current network status, controllers may not completely employ the available system capacity.

The distributed control methods utilize the limited communication links for data exchange between units to achieve control targets using maximum available facilities. In [20], a distributed method has been used for coordinated control of battery energy storage (BES) systems which solves the voltage rise/drop problem in LVDNs with high PV penetration. In this work, an identical power/capacity has been assumed for the batteries. The proposed leader-follower consensus algorithm in [20] has considered that the voltage at last bus of a radial feeder always will be the maximum/minimum voltage. However, if the last bus has small size PV system with relatively higher loads or a connection failure occurs in PV system, then the voltage of another bus will be higher/lower than the last bus voltage. Thus, the performance of control strategy can be degraded.

In the previous our work [21], a consensus-based distributed control strategy has been developed for fixed BES systems to regulate voltage in LVDNs with high penetration of PVs. This solution requires adding sufficient number and capacity of batteries in the PV systems. The proposed control scheme in [21] is based on a combination of the local and distributed control methods. A local droop-based control method initiates the weighted consensus algorithm to determine the BESs participation in terms of their installed capacity. Furthermore, the dynamic consensus algorithm modifies the BESs participation in terms of their state of charge (SoC). In [18], [20], and [21], a three-phase three-wire LVDN has been considered and the control method has been verified using a balanced network.

The main target of this paper is utilizing the energy storage capacity of available PEVs in residential networks instead of BESs for voltage regulation. Since the number of connected PEVs vary during voltage regulation, we have to choose appropriate consensus algorithms in the distributed method according to the requirements [21]. In addition, the control strategy should be able to recognize voltage violation at any bus to select it as the leader. We need also a supplementary method to help the main solution when the storage capacity of connected PEVs is not sufficient to store the excess PVs production. The single-phase loads, PV systems, and PEVs are not equally distributed among three phases of residential LVDNs. Thus, the control strategies should be designed to work properly for unbalanced four-wire systems.

C. Contributions

This paper contributes to the existing literature by proposing a distributed control strategy for coordinated charging/discharging of PEVs to regulate voltage in LVDNs with high penetration level of PV resources. The new proposed method is based on two consensus control algorithms to improve voltage profile along the feeder by coordinated employment of both battery storage of PEVs and APC of PV systems. The PEVs battery can be used to store a portion of the energy produced by PVs during peak generation periods and redistribute the stored energy into the network during peak load periods. If the voltage of a bus violates pre-defined limits, a leader-follower consensus algorithm determines the exchanged power between PEVs and the network proportional to the power/capacity of their battery. Simultaneously, an average consensus algorithm adjusts the output power of PEVs based on their SoC to prevent the early saturation/depletion and enable the effective utilization of available storage capacity throughout the network. This algorithm can calculate the average SoC of connected PEVs which are not fixed unlike the BESs in [21]. Since the number of available PEVs connected to the network is stochastic, sometimes there is not sufficient energy storage capacity for voltage rise mitigation during peak periods of PV generation. Therefore, a supplementary solution is added to support the main strategy in cases that available PEVs are deficient in capacity to prevent voltage rise completely. In such conditions, another leader-follower consensus algorithm is implemented to apply the fair APC to PV systems. These three parts together help to improve voltage profile of the LVDN.

We demonstrate the feasibility of our control algorithm through a case study in which the power/capacity and SoC of PEVs are different according to real world. The control algorithm is designed such that the PEVs have plug and play capability which means they can be arbitrarily disconnected from the network whenever the PEV owner is going to drive somewhere and connected again after returning to home in order to contribute to voltage regulation. More specifically, the control method is designed to apply on an unbalanced four-wire LVDN. In our proposed method, for more generality, each bus that experiences voltage limits violation is selected as the critical bus to start the control algorithm. Then, feasibility analysis of the proposed method is done for distribution networks with different sizes. Finally, the impact of voltage control is investigated on other network constraints including the voltage unbalance and the loading of the transformer and lines constructing the feeder. The main contributions of this paper are as follows:

- Employing two consensus-based distributed control algorithms for energy management of available PEVs and APC of PV systems in order to mitigate voltage rise/drop problem in an LNDN with high PV penetration.
- Determining the amount of PEVs power that should be exchanged with the network considering the power/capacity and SoC of their battery to effectively utilize the available energy storage capacity without adverse effect on owners' comfort by providing the plug and play capability of PEVs.

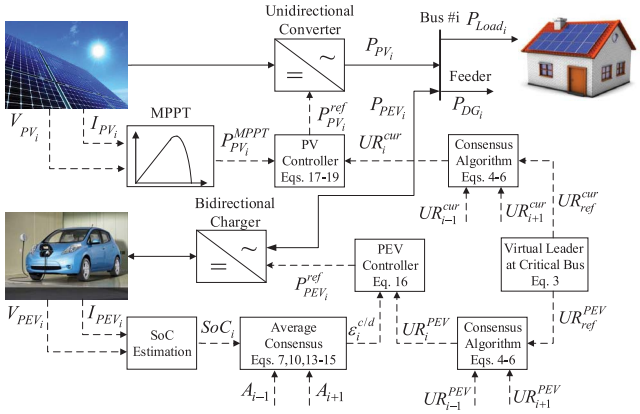

Fig. 1. Block diagram of the proposed control strategy for *i*th bus.

- Supporting the primary voltage regulation method of energy storage in PEV battery by the APC technique in the case of lacking a sufficient storage capacity during peak periods of PV generation.
- Modifying the leader-follower consensus algorithm in order to handle the cases in which the leader agent might be changed in different conditions.
- Designing the control method for three-phase four-wire LVDNs with unbalanced PV and load connections and then, investigating the impact of the proposed voltage control method on other network constraints, as well as it's feasibility for networks with different sizes.

This paper is organized as follows. In Section II, the proposed control method is presented. The test distribution system and necessary data are introduced in Section III. In Section IV, the simulation results are provided and Section V is devoted to drawing the conclusions.

II. Proposed Control Strategy

In this section, a new method to control the charging/discharging rate of PEVs battery and APC of PV systems is presented that regulates voltage in an LVDN. The block diagram of the proposed control strategy for the PEV and PV located at the *i*th bus is shown in Fig. 1. The solid and dotted lines show the power flow and control signal, respectively. The PV array is connected to the bus through a dc/ac converter. In addition, a bidirectional converter connects the PEV to the network to enable power exchange. The PV control is gained based on maximum power point tracking (MPPT) algorithm. Active power injection from the PV array would be limited by storing the extra power in the PEV battery which mitigates the voltage rise problem. In overvoltage conditions, it might be also required to employ the APC method. Moreover, during peak load periods, the stored energy in PEV battery can be utilized to compensate the voltage drop along the feeder.

As seen in Fig. 1, the utilization ratio control signal (UR_i) is determined by a consensus algorithm. The control signal is used to adjust the percentages of PEV power exchange with the network (UR_i^{PEV}) or the APC of PV (UR_i^{cur}). Moreover, the control signal ε_i is provided simultaneously by the average consensus algorithm to coordinate the SoC of PEVs battery.

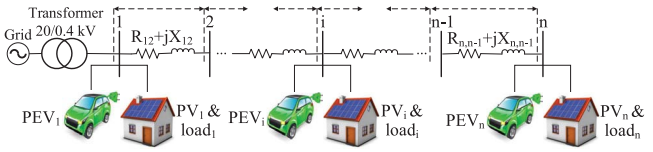

Fig. 2. A distribution feeder with PV and PEV systems and communication network.

Therefore, the exchanged power of each PEV is determined based on UR_i^{PEV}, $\varepsilon_i^{c/d}$, and its nominal power while the APC of each PV is calculated according to UR_i^{cur} and its injection power, if needed. The proposed control scheme is discussed in detail in the following subsections.

A. Coordination Between Charging/Discharging of PEVs Proportional to the Batteries' Power/Capacity

In this subsection, a consensus algorithm for distributed voltage control strategy is proposed which provide coordinated charging/discharging of available PEVs in the LVDN and to avoid APC of PVs generation as much as possible. The algorithm is applied to each phase of the three-phase four-wire LVDN separately. For example, Fig. 2 shows the phase *a* of an LNDN with *n* residential customers. It is assumed that each customer has both rooftop PV and PEV systems. The communication network structure associated with the proposed distributed control is shown in Fig. 2, where the dotted lines denote the data exchange among customers. In this scheme, a virtual leader is responsible for initiating the consensus algorithm by measuring the critical bus voltage. The last bus at the end of a radial feeder is usually considered as the critical bus [20], [22]. Here, for more generality, any of the buses which experiences voltage limits violation is selected as the critical bus to initiate the charging/discharging of PEVs. Therefore, all the buses can play the virtual leader role in the proposed algorithm and accordingly the other network buses will follow the leader to provide voltage regulation.

The state of each PEV is specified by the utilization ratio (UR_i^{PEV}) which is determined through the voltage measured at the critical bus. Then, UR_i^{PEV} is shared among the available PEVs in the network through communication links to adjust the output power of PEVs and achieve the desired voltage regulation. Firstly, it is aimed at designing a control method for UR_i^{PEV} such that the critical bus voltage is kept lower/higher than V_{thr}^c/V_{thr}^d during voltage rise/drop periods

$$V_{thr}^d \le v_{cri}(t) \le V_{thr}^c \tag{1}$$

where $v_{cri}(t)$ is the critical bus voltage. Moreover, V_{thr}^c and V_{thr}^d are the threshold voltages to initiate the charging and discharging of PEV, respectively. To avoid over/under voltage conditions, the threshold voltages should be selected within the allowed minimum/maximum limits of the network (V_{min}/V_{max}).

Secondly, the proposed control strategy aims to calculate a utilization ratio for each PEV (UR_i^{PEV}) such that Eqs. (2) are satisfied in the equilibrium point.

$$\frac{P_{PEV_i}}{\alpha_i \times P_{PEV_i}^{max}} = \frac{P_{PEV_{cri}}}{\alpha_{cri} \times P_{PEV_{cri}}^{max}} \quad i = 1, \ldots, n \setminus cri \tag{2}$$

where P_{PEV_i} and $P_{PEV_i}^{max}$ are the real time exchanged power between the PEV and the network and the maximum allowed power that the PEV can provide, respectively. Moreover, n denotes the number of agents (buses) in the distribution network. The weighting factor α_i adjusts the PEV's contribution to voltage regulation process. The batteries with larger capacity will have a larger weighting factor. The active power required for voltage regulation during voltage rise/drop periods will be shared among PEVs proportional to their battery capacity accordingly. Therefore, the higher storage capacity of the PEV battery leads to more PEV's contribution to voltage regulation.

To achieve the aforementioned goals, a bus is selected as the virtual leader and initiates the consensus algorithm, when its voltage violates the limits in (1). The state of virtual leader, UR_{ref}^{PEV}, is updated in discrete time steps as follows

$$UR_{ref}^{PEV}(t) = \begin{cases} UR_{ref}^{PEV}(t-\Delta t)+ & \\ k_v^d(v_{cri}(t) - V_{thr}^d) & v_{cri}(t) < V_{thr}^d \\ 0 & V_{thr}^d \le v_{cri}(t) \le V_{thr}^c \\ UR_{ref}^{PEV}(t-\Delta t)+ & \\ k_v^c(v_{cri}(t) - V_{thr}^c) & v_{cri}(t) > V_{thr}^c \end{cases} \tag{3}$$

where Δt is the sampling time period. k_v^c and k_v^d are constant parameters that adjust the convergence speed and accuracy of the control method.

The state of PEVs (UR_i^{PEV}) are communicated between neighbor units to update the utilization ratio of ith PEV

$$UR_i^{PEV}(t) = \sum_{j=1}^{n} w_{ij}(t) UR_j^{PEV}(t-\Delta t) \tag{4}$$

where $w_{ij}(t)$ is the (i,j) entry of a row stochastic matrix $W(t)$ in which the entries are calculated for a given discrete time step as follows

$$w_{ij}(t) = \frac{s_{ij}(t-\Delta t)}{\sum_{k=1}^{n} s_{ik}(t-\Delta t)} \tag{5}$$

where s_{ij} are the communication matrix entries, given as

$$S(t) = \begin{bmatrix} s_{11}(t) & s_{12}(t) & \dots & s_{1n}(t) \\ s_{21}(t) & s_{22}(t) & \dots & s_{2n}(t) \\ \vdots & \vdots & \ddots & \vdots \\ s_{n1}(t) & s_{n2}(t) & \dots & s_{nn}(t) \end{bmatrix} \tag{6}$$

Here, s_{ij} denotes the communication link between ith and jth buses. $s_{ij} = 1$ if jth bus sends data to ith bus, and $s_{ij} = 0$ otherwise. Moreover, $s_{ii} = 1$ for all i. In this paper, we assume that the buses can only communicate with their neighbors.

B. Coordination Between Charging/Discharging of PEVs Proportional to the Batteries' SoC

The introduced strategy in Section II-A is devised based on battery power/capacity of PEVs without considering their SoC. In practice, the SoC of PEVs batteries which are connected to the network will be different due to the difference existing in the number of travels and the distance driven per day. In the case of using only the power/capacity based control method, some PEVs may be fully charged/discharged in the process of voltage regulation due to the unpredictable pattern of daily travels. As a result, the contribution capability of some PEVs to voltage regulation would be decreased owing to their excessive charging/discharging. Therefore, modifying the voltage regulation method is necessary to maximize the utilization of batteries capacity. To this end, an average consensus control algorithm is added to the controller proposed in Section II-A in order to adjust the PEV charging/discharging rate such that the available storage capacity can be utilized more effectively.

The main idea of the average consensus algorithm is to estimate the average SoC of all PEVs battery connected to the network in a distributed manner such that occasional arrival/departure of PEVs do not affect the performance of control algorithm and PEVs have plug and play capability. Then, a contribution correction factor is calculated using the average SoC which modifies the exchanged power to keep the energy levels of the PEVs battery close together as far as possible.

The average consensus algorithm shares the local information of each agent in a distributed manner through which the agents can obtain the required information of the network. Here, each bus is considered as an agent. The information discovery law is defined as

$$x_i[k+1] = x_i[k] + \sum_{j \in N_i} d_{ij}\big(x_j[k] - x_i[k]\big) \tag{7}$$

where $i = 1, \dots, n$. $x_i[k]$ and $x_i[k+1]$ are the discovered information by the agent i at the k and $k+1$ iterations, respectively. d_{ij} is the communication coefficient between the neighbor agents i and j and N_i is the set of neighbor agents connected to agent i.

The information discovery law for the whole system can be modeled as a discrete time linear system

$$X[k+1] = DX[k] \tag{8}$$

where $X[k] = [x_1[k], \dots, x_i[k], \dots, x_n[k]]^T$ and $X[k+1]$ are the discovered information vector at the k and $k+1$ iterations, respectively, and D is a communication matrix. If the sums of D's rows and columns are equal to one and the eigenvalues of D satisfy $|\lambda_i| \le 1$, then it can be proved that [23]

$$\lim_{k\to\infty} X[k] = \lim_{k\to\infty} D^k X[0] = \frac{I.I^T}{n} X[0] \tag{9}$$

where I is a vector in which all of the entries equal 1 and $X[0]$ is the initial value of X. Eq. (9) shows that the speed of the information discovery process is determined by D. As discussed in [23], there are different methods for d_{ij} selection that give different convergence speed. In this paper, the *mean metropolis* method [23] is adopted with the following law

$$d_{ij} = \begin{cases} 2/\big(n_i + n_j + 1\big) & j \in N_i \\ 1 - \sum_{j\in N_i} 2/\big(n_i + n_j + 1\big) & i = j \\ 0 & otherwise \end{cases} \tag{10}$$

where n_i and n_j are the numbers of agents connected to agents i and j, respectively. Since it may take too long to reach the

exact equilibrium, a stopping criterion should be defined. To this aim, we define the error at kth iteration as [24]

$$E[k] = \| X[k] - X[\infty] \| = \| \left(D^k - J\right) X[0] \| \leq \| D - J \|^k \| X[0] - JX[0] \| \quad (11)$$

where $E[k]$ is the error at kth iteration and $J = \lim_{k\to\infty} D^k = \frac{1.1^T}{n}$. If a pre-defined precision requirement is considered to reach a consensus, the required number of iterations for convergence is approximately determined by [24]

$$K = \frac{1}{\log_{\frac{1}{E}}\left(\frac{1}{\|D-J\|}\right)} = \frac{-1}{\log_E\left(\frac{1}{|\lambda_2|}\right)} \quad (12)$$

where E is the error tolerance and λ_2 is the second largest eigenvalue of D. According to (12), it can be seen that λ_2 decides the convergence speed and imposes the approximate number of iterations for decreasing the error less than E. Eq. (12) indicates that the size of system does not influence the convergence speed but it is decided by the way the buses are connected and how D's elements are selected. Moreover, the algorithm is independent of initial values. Therefore, λ_2 can be used for evaluation of convergence speed.

According to (9), the average of different quantities (X) can be obtained in a distributed manner. The number of available PEVs in the network and their SoC are required to calculate the average SoC of batteries. To obtain this information, each agent is initialized with an $A_{n\times 2}$ matrix. In matrix A, only the rows corresponding to the agents' number can have nonzero elements. $A(i, 1)$ can be equal to either 1 or 0 to represent whether the PEV of agent i is connected or not. Moreover, if the PEV owner does not allow the PEV battery to contribute to voltage regulation for any reason, the corresponding element will equal zero. In the case of having a PEV connected to the agent i which contribute to the voltage regulation process according to the owner decision, $A(i, 2)$ is equal to its battery SoC, and zero otherwise. For example, if the ith PEV can contribute to voltage regulation, the ith row of its A matrix is initialized with [1 SoC_i]. Conversely, if the PEV is not connected to bus i, the corresponding row is [0 0].

By applying the information discovery algorithm (7) to each initial matrix, all the information matrices will converge to a same matrix where each element is the average summation of the corresponding elements in the initial matrices. For further explanation, a case with the connected PEVs at buses 1 and n is considered while there is no PEV connected to other buses. Thus, the initial and converged matrices are as

$$\begin{bmatrix} 1 & SoC_1 \\ \vdots & \vdots \\ 0 & 0 \\ \vdots & \vdots \\ 0 & 0 \end{bmatrix} \cdots \begin{bmatrix} 0 & 0 \\ \vdots & \vdots \\ 0 & 0 \\ \vdots & \vdots \\ 0 & 0 \end{bmatrix} \cdots \begin{bmatrix} 0 & 0 \\ \vdots & \vdots \\ 0 & 0 \\ \vdots & \vdots \\ 1 & SoC_n \end{bmatrix} \Rightarrow \begin{bmatrix} 1/n & SoC_1/n \\ \vdots & \vdots \\ 0 & 0 \\ \vdots & \vdots \\ 1/n & SoC_n/n \end{bmatrix}$$

The number of PEVs connected to the network can be found by counting the nonzero elements in the first column of the final converged matrix. The ratio of the second column summation to the first column summation determines the average SoC of PEVs battery

$$\overline{SoC_i} = \frac{\sum_{j=1}^{n} A(j, 2)}{\sum_{j=1}^{n} A(j, 1)} \quad (13)$$

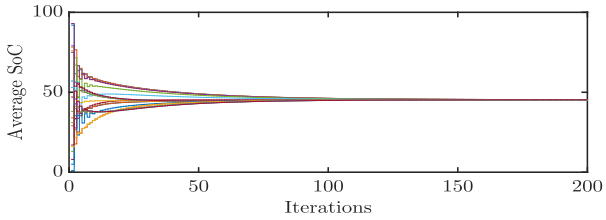

Fig. 3. Estimation of average SoC using average consensus control algorithm.

In this way, each agent updates its initial information matrix after the arrival or departure of the PEV. Moreover, the average SoC is estimated after multiple iterations of average consensus algorithm within a short time. For example, the process of estimating the average of SoC for 21 PEV is demonstrated in Fig. 3 where the SoCs have been initialized by being set equal to random values. As it can be seen, after running 160 iterations, all the estimated $\overline{SoC_i}$ converge to a consensus value which is the true average of the SoCs in the network.

After estimating the average SoC, the contribution correction factor of the PEVs in charging/discharging mode ($\varepsilon_i^c/\varepsilon_i^d$) is calculated based on the defined control rules in (14) and (15) in order to maintain the corresponding SoC uniform

$$\varepsilon_i^c = \begin{cases} 0 & SoC_i > SoC_i^{max} \\ 1 - k_{SoC}^c\left(\frac{SoC_i - \overline{SoC_i}}{100}\right) & SoC_i \leq SoC_i^{max} \end{cases} \quad (14)$$

$$\varepsilon_i^d = \begin{cases} 1 + k_{SoC}^d\left(\frac{SoC_i - \overline{SoC_i}}{100}\right) & SoC_i \geq SoC_i^{min} \\ 0 & SoC_i < SoC_i^{min} \end{cases} \quad (15)$$

where k_{SoC}^c and k_{SoC}^d are constant parameters which adjust the convergence speed of SoCs in charging and discharging modes, respectively. SoC_i^{min} is the minimum required energy level of PEV for the next travel specified by the owner and SoC_i^{max} is the maximum allowed energy level of battery determined by technical limitations. For further explanation of the control logic, consider (14) that calculates the ε_i^c. If real time battery energy level (SoC_i) is lower than the estimated average SoC ($\overline{SoC_i}$), then $\varepsilon_i^c > 1$. This means that the PEV contribution should be increased during charging mode. Conversely, if $SoC_i > \overline{SoC_i}$, then $\varepsilon_i^c < 1$ and the energy absorption by PEV should be decreased. It should be noted that if the SoC of a PEV battery violates the pre-defined allowed limits (SoC_i^{max}/SoC_i^{min}) during charging/discharging modes, the PEV will be removed from the voltage regulation process.

Finally, the exchanged power of a PEV located at bus i is given by

$$P_{PEV_i}^{ref} = \varepsilon_i^{c/d} \times UR_i^{PEV} \times \alpha_i \times P_{PEV_i}^{max} \quad (16)$$

where $P_{PEV_i}^{ref}$ is the charging/discharging power of the ith PEV.

C. APC Coordination of PVs Proportional to Net Injection

When there is not sufficient energy storage capacity due to either the limited numbers of PEVs connected to the network

or the available batteries which are charged up to their maximum allowed limit, the APC method is added to the algorithm to prevent overvoltage during peak generation periods. The UR_{ref}^{PEV} calculated for the critical bus is used to initiate this supplementary method. When the virtual leader experiences overvoltage and UR_{ref}^{PEV} equals 1, it indicates that all the capacity of the available batteries have been fully used and there is no storage capacity to absorb the extra energy produced by PVs. In this case, the virtual leader runs a distributed algorithm similar to the one introduced in Section II-A for curtailing the power injected by PVs, and thus, the algorithm must be run separately for three phases.

This part of the algorithm aims at curtailing the PV output power proportional to the real time net injection so that the customers fairly contribute to voltage regulation. Hence, larger power curtailment should be assigned to the customers with higher net power injection into the network. Therefore, the utilization ratio UR_i^{cur} of each PV is determined such that Eqs. (17) are satisfied in the equilibrium point.

$$\frac{P_{PV_i}^{cur}}{P_i^{net}} = \frac{P_{PV_{cri}}^{cur}}{P_{cri}^{net}} \quad i = 1, \ldots, n \setminus cri \tag{17}$$

where $P_{PV_i}^{cur}$ is the curtailed power of PV_i and P_i^{net} is the real time net injection at ith bus, respectively. The remaining parts are similar to those provided in (3)-(6) and thus they are not repeated here. This method calculates a UR_i^{cur} for each PV that is multiplied by P_i^{net} to obtain the curtailed power

$$P_{PV_i}^{cur} = UR_i^{cur} \times P_i^{net} \tag{18}$$

Therefore, the power generation reference for PV_i is

$$P_{PV_i}^{ref} = P_{PV_i}^{MPPT} - P_{PV_i}^{cur} \tag{19}$$

where $P_{PV_i}^{MPPT}$ is the power calculated by MPPT algorithm.

D. Discussion

The proposed consensus control algorithm in Section II-A shares the required power exchange for voltage regulation proportional to power/capacity of PEVs battery without considering the energy level of batteries. Thus, it is expected that the PEVs with higher SoC will become full in the charging mode and they can no longer contribute to overvoltage mitigation during periods of peak PV generation. Furthermore, the remained batteries may not be able to provide the required power. Similarly, once a battery runs out of energy, it can not supply energy during peak load periods which leads to degrading the voltage regulation process. Therefore, in order to prevent PEVs from early running out of service in charging/discharging mode, the power/capacity based control strategy must be improved to consider the energy level of PEVs battery. On the other hand, if batteries power is exchanged only based on their SoC, when some batteries absorb less power due to running full of energy, the capacity of other PEVs with lower SoC may be less than the required power for effective voltage regulation.

Consequently, in the first step of the process, the required power exchange of PEVs during voltage rise/drop period is determined based on power/capacity of their battery. Then, an average consensus control algorithm is applied to prevent early saturation/depletion of the batteries. The active power curtailment of PV systems also helps the voltage regulation process at necessary times. The combined control strategy presents an improved performance in comparison to only considering the PEV power/capacity or SoC.

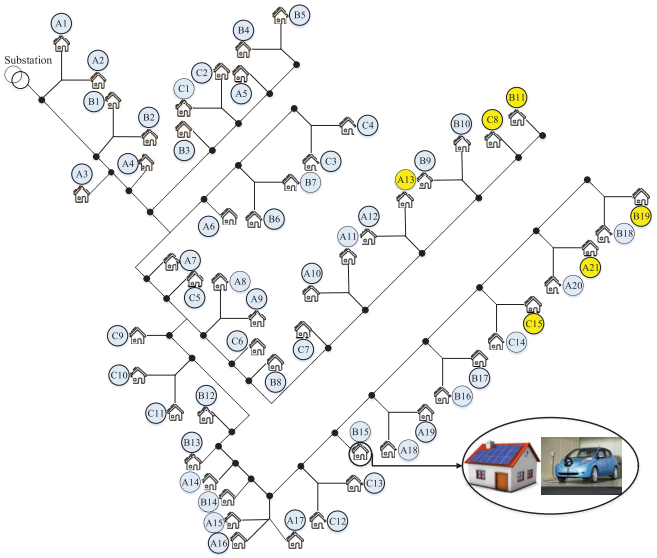

Fig. 4. The IEEE European LV test feeder.

TABLE I
PARAMETERS OF PROPOSED CONTROL METHOD

Charging/Discharging Threshold Voltages		Consensus Algorithm Coefficients		Average Consensus Algorithm Coefficients	
V_{thr}^{c}	V_{thr}^{d}	k_v^c	k_v^d	k_{SoC}^c	k_{SoC}^d
1.05 p.u.	0.95 p.u.	0.005	0.005	5	5

III. TEST NETWORK AND DATA

A. Residential Low Voltage Distribution Network

The IEEE European LV test feeder [26] shown in Fig. 4 is modeled in MATLAB/Simulink to assess the effectiveness of the proposed control strategy. This feeder supplies 55 single-phase customers through an 800 KVA, 11 kV/416 V transformer. The radial three-phase four-wire network consists of 21, 19, and 15 customers spread across phases *a*, *b*, and *c*, respectively. The impedance characteristics of distribution lines and their length have been provided in [26]. Moreover, the maximum allowed voltage deviation along the feeder is assumed 0.05 p.u. The parameters of control algorithms are given in Table I. The simulation is run using the phasor solution technique [27], as the changes in amplitude of voltages are only needed to evaluate the proposed method. These changes can be calculated by solving a set of algebraic equations relating the voltage and current phasors.

B. Load Data and Residential Rooftop PV Profiles

The typical residential load profiles in [28] have been used for simulations which were assigned to the houses randomly. The load type is the constant power with a power factor of

TABLE II
PEV SPECIFICATIONS

Type	Battery Capacity (kWh)	Charger Power (kW)	Weighting Coefficient (α)	Energy Consumption (kWh/km)
1	30	3.3	1	0.2
2	24	3.3	0.8	0.2

0.95. A 4 kW rooftop PV array has been installed in each house which is operated in unity power factor by MPPT algorithm. The measured data of 20 kW solar plant at Isfahan University of Technology in the winter 2015 have been used as the PV output profiles [21]. The PV profiles were rescaled proportional to the size of the corresponding inverter. Since the geographical area was small, we have considered identical output power profile of all PVs. The PV and load profiles are characterized as 5-minute data. The PV and load data are also scaled up for this application and they hold the same value for every 5 minutes to cope with the simulation speed.

C. PEV Data and Travel Pattern

It is assumed that every house has one PEV. In addition, two PEV battery types with specifications given in Table II are employed [29]. We have assumed that each type is used by half of the vehicles. The minimum SoC of the PEV battery is determined by owners based on average daily travel (e.g., 30 km) that is considered 30% for both battery types.

IV. RESULTS AND ANALYSIS

The proposed control algorithm is run separately for each phase of LVDN. Therefore, a critical bus should be considered as the virtual leader for each phase. Whenever the measured voltage of a bus violates the allowed limits, it is selected as the critical bus. The selected bus is the virtual leader for other buses in voltage regulation process. For radial LVDNs, the last bus usually experiences maximum voltage deviation during voltage rise/drop period. For example in Fig. 4, A13/A21, B11/B19, and C8/C15 can be considered as the virtual leaders for phases *a*, *b*, and *c*, respectively. Due to the space limitation, the impacts of the proposed control strategy on the LVDN voltage regulation are studied mainly based on phase *a*, which has more PV and load than those of the other phases.

Several simulation scenarios have been defined to analyze the performance of the proposed voltage regulation method. To mitigate the voltage rise/drop problem using PEVs battery, an adequate energy storage capacity is required to be considered in the network. The statistics presented in [14] indicate that there is about 50% probability for a PEV to be parked at a house during a peak PV generation period. Accordingly, the first scenario assumes 47% PEV penetration for each phase in LVDN. In this case, there is an adequate storage capacity to prevent overvoltage due to the extra power injected by PVs. Therefore, the supplementary method of APC is not employed. The impacts of occasional arrival/departure of PEVs at/from the houses and plug and play capability are investigated in the second scenario. The duration of travels, the distance driven before returning to the parking, and the arrival/departure times

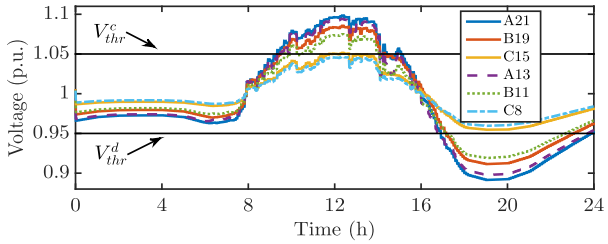

Fig. 5. The 24-hour voltage profiles of critical buses.

of PEVs are determined randomly. Since the PEV penetration of the first scenario is overestimated, the penetration level is reduced to about 25% in the third scenario. In this case, due to the lack of the adequate storage capacity, a combination of PEV charging/discharging and APC control methods is used. Then, feasibility analysis of the proposed method for distribution networks with different sizes is done. Finally, the last study is devoted to investigating the impact of voltage control on other network constraints.

A. First Scenario: 47% Penetration of PEV

Consider a scenario where the number of parked PEVs at houses for phases *a*, *b*, and *c* are 10, 9, and 7, respectively that leads to a 47% penetration. At first, for simplicity, all PEVs are assumed to be connected to the network during voltage regulation period and not to leave the parking for travel. Figure 5 shows the voltage profiles at critical buses of the network when the PVs are controlled in MPPT mode without any voltage control. As can be observed, the reverse power flow leads to the voltage rise at midday and the peak loads result in voltage drop in the evening. Therefore, the voltage violates the allowed limits during the above-mentioned periods.

In the next study, the voltage control algorithm using PEVs battery is activated by applying both consensus algorithms introduced in Section II. The voltage profiles of critical buses are shown in Fig. 6a accordingly. It is observed that the maximum and minimum voltages are kept within a pre-defined allowed limits to make the designed voltage controller work appropriately. Figures 6b–6d show the 24-hour SoC profiles of PEVs battery for three phases of the test network. Despite the difference among the initial values of SoCs, the average consensus algorithm reduces the existing discrepancy and consequently, the SoC of all batteries converge together in charging/discharging mode.

The utilization ratio of the PEVs battery (UR^{PEV}) for three phases are shown in Fig. 7. The consensus control algorithm introduced in Section II-A determines the UR^{PEV} so that all PEVs satisfy the defined ratio in (2) and exchange power with the network accordingly. For larger capacity of the PEV battery, a larger α coefficient is assigned and thus, it has more contribution to voltage regulation. This is due to the fact that in this case the battery must absorb/inject more power according to (2). As it can be seen, phase *a* has higher utilization ratio of the capacity of PEVs battery compared to that of other phases. This occurs due to the fact that the more customers are connected to phase *a* and thus, it has higher PV generation and load consumption in comparison with other two phases.

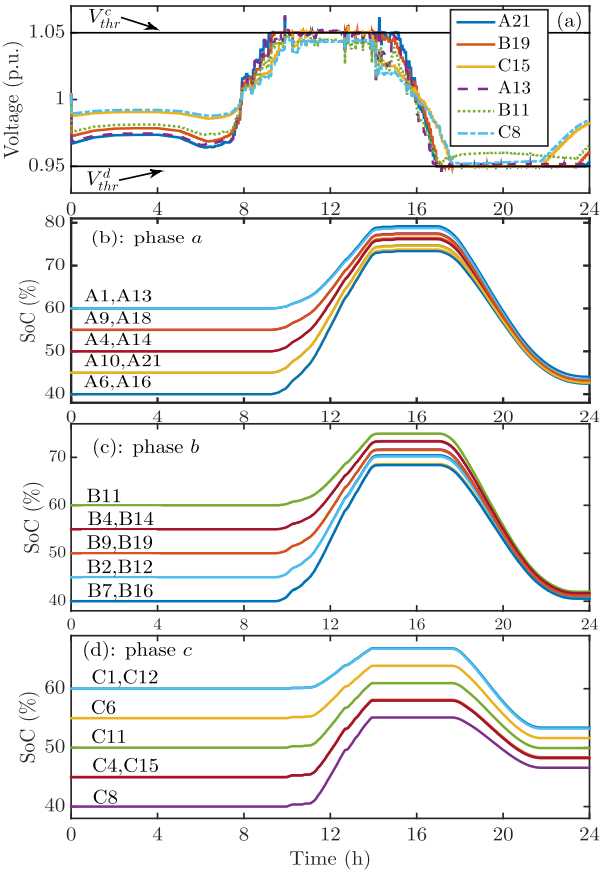

Fig. 6. Coordinated charging/discharging control of PEVs for voltage regulation. (a) voltage profile; (b) SoC of batteries at phase *a*; (c) SoC of batteries at phase b; (b) SoC of batteries at phase c.

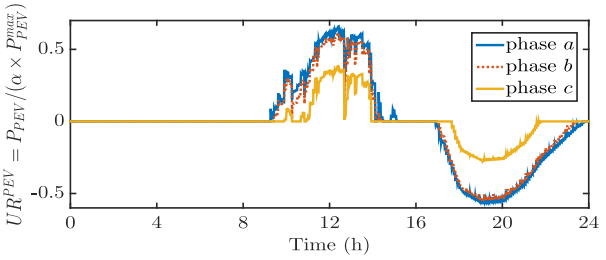

Fig. 7. The utilization ratio of each phase.

To illustrate the necessity of applying two consensus algorithms simultaneously (as discussed in Section II-D), a simulation was conducted without the average consensus algorithm. All other conditions are as the same as previous except the initial SoCs which have been raised %10. In this case, the SoC of PEVs does not influence the charging/discharging rate. The 24-hour voltage profiles of the critical buses and SoC variations of connected PEVs to phase *a* are shown in Figs. 8a and 8b, respectively. Since the batteries are controlled proportional to their power/capacity, SoCs also change almost uniformly. However, as seen in Fig. 8a, the maximum voltage limit is violated during peak PV generation period. This is due to the fact that as the power absorption by some PEVs (A1,9,13,18) decrease due to running full of energy, the capacity of remaining PEVs with lower SoC is less than the required

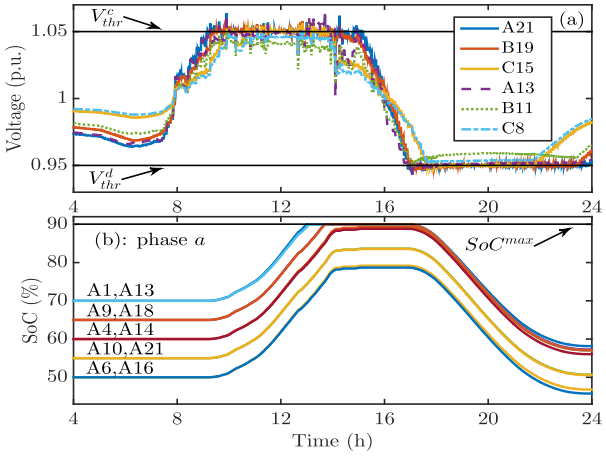

Fig. 8. Coordinated control scheme without the average consensus algorithm. (a) voltage profile; (b) SoC of batteries at phase *a*.

TABLE III
TRAVEL SCHEDULE OF PEVS AT PHASE *a* DURING PEAK PV GENERATION AND PEAK LOAD PERIODS

PEV Number	A1	A4	A6	A9	A16	A18
Travel Time (h)	12:00-13:00	20:30-21:00	19:00-20:00	11:00-11:30	18:00-18:30	13:30-14:00
Energy Consumption (%)	20	10	20	10	10	10

power for voltage control. Therefore, the combined control strategy consists of both consensus algorithms must be used for better performance.

B. Second Scenario: Investigating the Impacts of Occasional Arrival/Departure of PEVs

Now, the impacts of occasional arrival/departure of PEVs during a day due to the short-time travels are studied. Table III specifies the travel schedule of the PEVs connected to phase *a*. Considering the batteries specifications and the estimated distance driven during each travel, the required energy for 30 min and one hour travels is assumed to be 10% and 20% of stored energy in PEV battery, respectively.

The study results of phase *a* are illustrated in Fig. 9. As the voltage profiles at buses A13 and A21 in Fig. 9a demonstrate, the allowed voltage limits are not violated and thus, it can be concluded that other buses of phase *a* will not experience a voltage rise/drop. Despite the occasional arrival/departure of PEVs during voltage rise/drop periods, Fig. 9b shows that the average consensus algorithm performs as desired and it can maintain the SoC convergence of batteries to efficiently utilize the available storage capacity. Moreover, the results indicate that the control algorithm is robust against plug and play nature of PEVs. Therefore, the proposed control scheme presents plug and play capability such that the occasional travels of PEVs do not influence the target of voltage control. It should be noted that the SoC of the PEVs which are outside of the parking is not considered in the estimation process of the average SoC and assumed to remain unchanged.

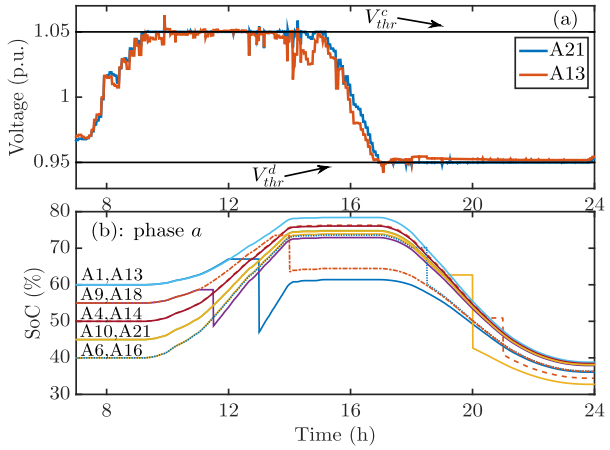

Fig. 9. The impact of PEVs arrival/departure. (a) voltage profile at critical buses of phase *a*; (b) SoC variations of PEVs battery.

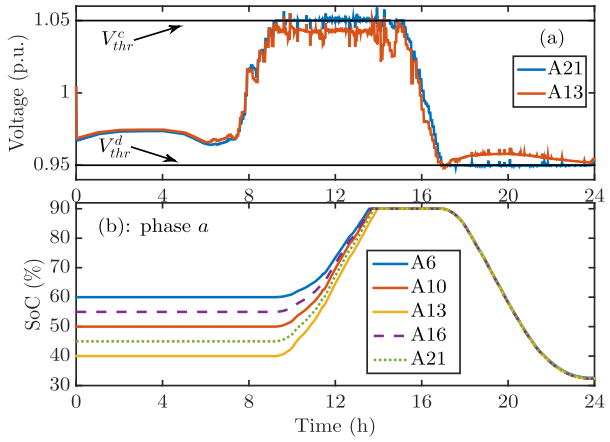

Fig. 10. The results of third scenario. (a) 24-hour voltage profile; (b) SoC variations of PEVs battery.

C. Third Scenario: 25% Penetration of PEV

This subsection assumes lower number of PEVs (25% penetration) parked at houses during peak PV generation period in comparison with the first scenario. This scenario is designed to investigate the performance of the proposed control method when there is not adequate storage capacity for absorbing the extra power of PVs and also to prevent overvoltage in the network. As a result, the combined method of energy storage and APC is used for voltage regulation process.

Figures 10a and 10b show the voltage profile at critical buses and the SoC variations of available PEVs battery at phase *a*, respectively. The maximum and minimum pre-defined limits of voltage are not violated and the coordinated charging/discharging process of available PEVs is run appropriately. As depicted in Fig. 10b, the energy level of all PEVs reaches its maximum allowed limit (90%) before the end of overvoltage period and the energy storage capacity converges to zero. Therefore, according to the method introduced in Section II-C, the APC of PVs is activated by the consensus control algorithm to prevent overvoltage in the LVDN in a fair way. In this case, we assume that the number of PEVs suffices to compensate voltage drop during peak load periods. This is due

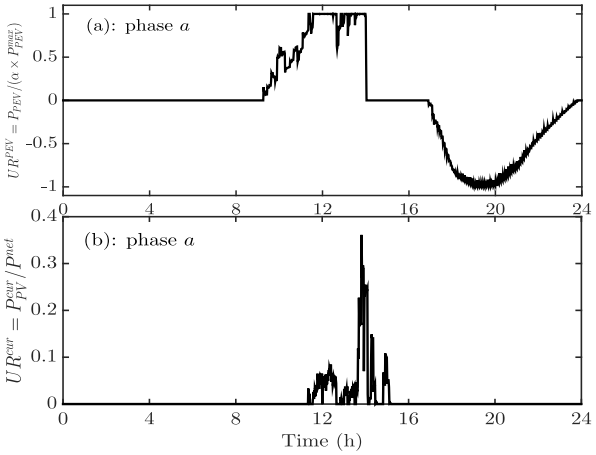

Fig. 11. The utilization ratios. (a) battery capacity of PEVs; (b) power curtailment of PVs.

to the fact that the PEVs which are likely charged in workplace, usually are returned home during peak load periods and the energy stored in their battery can be used to support the network. Furthermore, in order to increase the energy level for driving in the following day, the charging time of PEVs can be postponed until the late at night or the early morning. This strategy also prevents imposing additional stress on the network by PEVs charging during peak load periods.

The utilization ratios of PEVs battery capacity and PVs power curtailment are shown in Figs. 11a and 11b, respectively. It can be seen that UR^{PEV} reaches to the maximum value (i.e., 1) in 11.5 h, that is the maximum possible utilization of PEVs battery in the contribution to the voltage regulation process. Simultaneously, the UR^{cur} begins to increase in order to prevent overvoltage by curtailing the produced power of PV arrays. This proceeds within the overvoltage period about $15\frac{1}{4}$ h when UR^{cur} returns to zero. It should be noted that the coefficients are obtained identical for all PEVs and PVs in the phase *a*.

D. Feasibility Analysis for Larger Networks

As seen in Fig. 3, the convergence speed of the average consensus algorithm is evaluated using the number of iterations instead of time. Although the specifications of implemented software and hardware determines the time, a rough estimation is provided. The required time for algorithm convergence can be estimated as follows

$$t_{con} = \frac{n_{it} \times d_{im} \times n_b}{s_c} \tag{20}$$

where n_{it} is number of iterations for converging, d_{im} is the dimensions of information matrix D, n_b is the number of bits used to represent each element of D, and s_c is the communication speed in terms of Mbits/s. For example, as shown in Fig. 3, 160 iterations takes long to reach the convergence. Assuming a communication speed of 1 Mbit/s and each element of D is represented using 16 bits, t_{con} is calculated about 0.1075 s. Thus, the algorithm is fast enough for real-time control which is 5-minute time steps for updating the information matrices in our application.

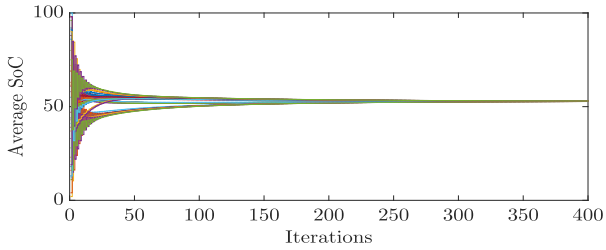

Fig. 12. Estimation of average SoC using average consensus control algorithm in IEEE 123-bus distribution network.

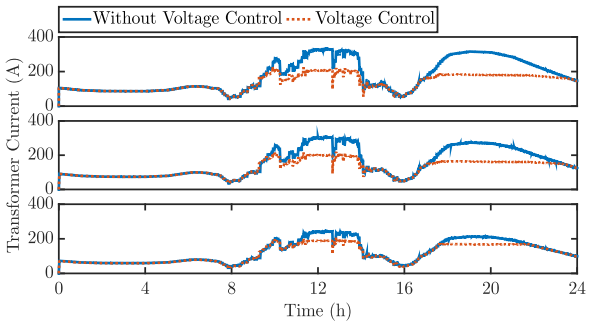

Fig. 13. Transformer current.

In this subsection, the average consensus algorithm is tested with the IEEE 123-bus distribution network [26] to investigate its performance when the problem size increases. The algorithm has been used for estimating the average SoC of PEVs battery connected to phase *a*. The information matrix is designed based on the *Mean Metropolis* method. According to (12), the estimated iterations needed for achieving consensus with tolerance 0.03 is 390, as illustrated in Fig. 12. In this case, the equivalent time is 0.2621 s which is sufficient.

E. Investigating Other Network Constraints

The effect of the proposed control strategy on the loading of the MV/LV transformer located at the beginning of the low voltage distribution feeder is shown in Fig. 13. As it can be seen, by applying the control method, the current amplitude of three phases of the transformer are reduced during voltage control periods. Fig. 14 shows the three-phase currents amplitude of the lines constructing the main feeder. The same as previous figure, we can conclude that the employed voltage control reduces the currents amplitude.

Furthermore, unsymmetrical generation and consumption at different phases lead to voltage unbalance which is one of the main limiting factors in distribution networks. To evaluate the voltage unbalance in three-phase networks, the voltage unbalance factor (VUF) is calculated as follows [17]

$$VUF(\%) = \frac{V_{inv}}{V_{dir}} \times 100 \tag{21}$$

where V_{inv} and V_{dir} are inverse and direct sequences of the voltage in symmetrical coordinates, respectively. The European standard EN50160 [30] defines acceptable limit of MV/LV distribution networks as VUF$\leq$ 2% for more than 95% of 10 min intervals during one week to ensure that electric appliances are operated in a safe manner.

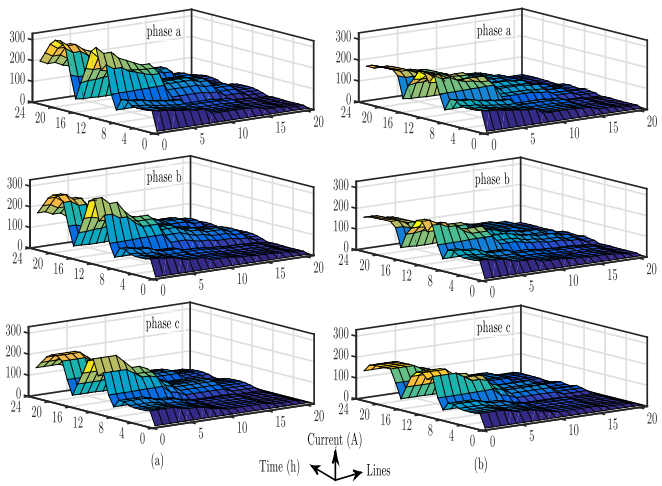

Fig. 14. Line currents. (a) Without voltage control; (b) Voltage control.

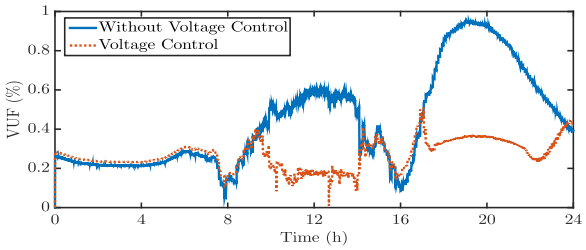

Fig. 15. VUF at bus C15.

The VUF was calculated for all buses of the test feeder. It was observed that VUF increases by moving towards the end of feeder. Bus C15 was recognized as the critical bus with the highest voltage unbalance. Fig. 15 shows the 24-hour profile of VUF for three-phase voltage measured at bus C15. It can be observed that voltage regulation also reduce the voltage unbalance of the network.

Since the line currents, transformer loading, and VUF are functions of three-phase bus voltages, voltage control of each phase within the acceptable limits close to each other can reduce them to minimum amounts.

V. Conclusion

This paper proposes a new voltage regulation strategy in low voltage distribution networks (LVDN) with high penetration of photovoltaic (PV) resources. The proposed control scheme presents a solution composed of energy storage in plug-in electric vehicles (PEV) battery and active power curtailment (APC) of PV system to address the voltage rise/drop problems in LVDNs. A coordinated control strategy has been developed using the consensus control algorithm to maximize the utilization of available PEVs storage capacity in the residential houses considering the power/capacity and state of charge (SoC) of their battery as well as to minimize the curtailment of PVs generation. The control scheme prevents early saturation/depletion of PEVs battery by adjusting the charging/discharging rate and also fairly shares the required APC among PVs. The simulation results verify that the proposed strategy is robust against occasional arrival/departure of PEVs while presenting plug and play capability for energy storage

devices. The algorithm is applicable to any configurations and sizes of distribution networks. Moreover, it is shown that voltage regulation can help to improve other network constraints such as loading and voltage unbalances.

REFERENCES

[1] H. A. Gil and G. Joos, "Models for quantifying the economic benefits of distributed generation," *IEEE Trans. Power Syst.*, vol. 23, no. 2, pp. 327–335, May 2008.

[2] J. A. P. Lopes, N. Hatziargyriou, J. Mutale, P. Djapic, and N. Jenkins, "Integrating distributed generation into electric power systems: A review of drivers, challenges and opportunities," *Elect. Power Syst. Res.*, vol. 77, no. 9, pp. 1189–1203, Jul. 2007.

[3] A. Zahedi, "Maximizing solar PV energy penetration using energy storage technology," *Renew. Sustain. Energy Rev.*, vol. 15, no. 1, pp. 866–870, Jan. 2011.

[4] J. García-Villalobos, I. Zamora, J. I. S. Martín, F. J. Asensio, and V. Aperribay, "Plug-in electric vehicles in electric distribution networks: A review of smart charging approaches," *Renew. Sustain. Energy Rev.*, vol. 38, pp. 717–731, Oct. 2014.

[5] M. K. Gray and W. G. Morsi, "Power quality assessment in distribution systems embedded with plug-in hybrid and battery electric vehicles," *IEEE Trans. Power Syst.*, vol. 30, no. 2, pp. 663–671, Mar. 2015.

[6] X. Liu, A. Aichhorn, L. Liu, and H. Li, "Coordinated control of distributed energy storage system with tap changer transformers for voltage rise mitigation under high photovoltaic penetration," *IEEE Trans. Smart Grid*, vol. 3, no. 2, pp. 897–906, Jun. 2012.

[7] S. Alyami, Y. Wang, C. Wang, J. Zhao, and B. Zhao, "Adaptive real power capping method for fair overvoltage regulation of distribution networks with high penetration of PV systems," *IEEE Trans. Smart Grid*, vol. 5, no. 6, pp. 2729–2738, Nov. 2014.

[8] F. Olivier, P. Aristidou, D. Ernst, and T. Van Cutsem, "Active management of low-voltage networks for mitigating overvoltages due to photovoltaic units," *IEEE Trans. Smart Grid*, vol. 7, no. 2, pp. 926–936, Mar. 2016.

[9] F. Marra, G. Yang, C. Traeholt, J. Ostergaard, and E. Larsen, "A decentralized storage strategy for residential feeders with photovoltaics," *IEEE Trans. Smart Grid*, vol. 5, no. 2, pp. 974–981, Mar. 2014.

[10] M. S. ElNozahy and M. M. A. Salama, "Uncertainty-based design of a bilayer distribution system for improved integration of PHEVs and PV arrays," *IEEE Trans. Sustain. Energy*, vol. 6, no. 3, pp. 659–674, Jul. 2015.

[11] S. Weckx and J. Driesen, "Load balancing with EV chargers and PV inverters in unbalanced distribution grids," *IEEE Trans. Sustain. Energy*, vol. 6, no. 2, pp. 635–643, Apr. 2015.

[12] J. Traube *et al.*, "Mitigation of solar irradiance intermittency in photovoltaic power systems with integrated electric-vehicle charging functionality," *IEEE Trans. Power Electron.*, vol. 28, no. 6, pp. 3058–3067, Jun. 2013.

[13] J. Tomić and W. Kempton, "Using fleets of electric-drive vehicles for grid support," *J. Power Sources*, vol. 168, no. 2, pp. 459–468, Jun. 2007.

[14] D. Wu, D. C. Aliprantis, and K. Gkritza, "Electric energy and power consumption by light-duty plug-in electric vehicles," *IEEE Trans. Power Syst.*, vol. 26, no. 2, pp. 738–746, May 2011.

[15] L. Cheng, Y. Chang, and R. Huang, "Mitigating voltage problem in distribution system with distributed solar generation using electric vehicles," *IEEE Trans. Sustain. Energy*, vol. 6, no. 4, pp. 1475–1484, Oct. 2015.

[16] J. M. Foster, G. Trevino, M. Kuss, and M. C. Caramanis, "Plug-in electric vehicle and voltage support for distributed solar: Theory and application," *IEEE Syst. J.*, vol. 7, no. 4, pp. 881–888, Dec. 2013.

[17] K. Knezović and M. Marinelli, "Phase-wise enhanced voltage support from electric vehicles in a Danish low-voltage distribution grid," *Elect. Power Syst. Res.*, vol. 140, pp. 274–283, Nov. 2016.

[18] M. J. E. Alam, K. M. Muttaqi, and D. Sutanto, "Effective utilization of available PEV battery capacity for mitigation of solar PV impact and grid support with integrated V2G functionality," *IEEE Trans. Smart Grid*, vol. 7, no. 3, pp. 1562–1571, May 2016.

[19] S. Weckx, R. D'Hulst, B. Claessens, and J. Driesensam, "Multiagent charging of electric vehicles respecting distribution transformer loading and voltage limits," *IEEE Trans. Smart Grid*, vol. 5, no. 6, pp. 2857–2867, Nov. 2014.

[20] Y. Wang, K. T. Tan, X. Y. Peng, and P. L. So, "Coordinated control of distributed energy-storage systems for voltage regulation in distribution networks," *IEEE Trans. Power Del.*, vol. 31, no. 3, pp. 1132–1141, Jun. 2016.

[21] M. Zeraati, M. E. H. Golshan, and J. Guerrero, "Distributed control of battery energy storage systems for voltage regulation in distribution networks with high PV penetration," *IEEE Trans. Smart Grid*, to be published.

[22] G. Mokhtari, A. Ghosh, G. Nourbakhsh, and G. Ledwich, "Smart robust resources control in LV network to deal with voltage rise issue," *IEEE Trans. Sustain. Energy*, vol. 4, no. 4, pp. 1043–1050, Oct. 2013.

[23] Y. Xu and W. Liu, "Novel multiagent based load restoration algorithm for microgrids," *IEEE Trans. Smart Grid*, vol. 2, no. 1, pp. 152–161, Mar. 2011.

[24] L. Xiao and S. Boyd, "Fast linear iterations for distributed averaging," in *Proc. 42nd IEEE Int. Conf. Decis. Control*, vol. 5. Dec. 2003, pp. 4997–5002.

[25] R. Olfati-Saber, "Algebraic connectivity ratio of Ramanujan graphs," in *Proc. Amer. Control Conf.*, New York, NY, USA, Jul. 2007, pp. 4619–4624.

[26] (May 2015). *The IEEE European Low Voltage Test Feeder*. [Online]. Available: http://ewh.ieee.org/soc/pes/dsacom/testfeeders/

[27] (2017). *Introducing the Phasor Simulation Method*. [Online]. Available: https://www.mathworks.com/help/physmod/sps/powersys/ug/introducing-the-phasor-simulation-method.html

[28] *OpenEI: Energy Information Datasets*. [Online]. Available: http://en.openei.org/datasets/files/961/pub/

[29] *2016 Nissan Leaf*. Accessed: Mar. 2016. [Online]. Available: https://www.nissanusa.com/ content/nissan-responsive/us/en/forms/

[30] H. Markiewicz and A. Klajn, *Voltage Disturbances*, EN Standard 50160, 2014.

Authors' photographs and biographies not available at the time of publication.